Research of cyclist's spine dynamical model

Julius Griskevicius[1]*, Arturas Linkel[1], JolantaPauk[2]

[1] Vilnius Gediminas Technical University, Vilnius, Lithuania.
[2] Białystok University of Technology, Białystok, Poland.

The purpose of the paper is to present a dynamic model of bicyclist's lumbar spine for the evaluation of linear and angular variation of intervertebral distance in sagittal plane. Ten degrees of freedom biomechanical model of the spine was solved numerically. Larger loads acting on a cyclist spine occur mostly while sitting in a sport position in comparison with recreation or middle sitting. The load on lumbar spine region is influenced by cycle's tire pressure, road bumps and wheeling speed. The biggest linear and angular displacements were found between L4–L5 vertebras. The biggest load protractile spine muscle experiences in the sport sitting position. Maximum vertebrae rotation and linear variation values in wheeling regime with 1.5 Bar tyres pressure and at a speed of 10 km/h are 0.46° and 0.46 mm. Maximum vertebrae rotation and linear variation values for a 23 year old, 1.74 m high and 73 kg of mass (bicycle mass ~ 7 kg) man in wheeling regime with 3.5 Bar tyres pressure and at a speed of 30 km/h are 3.9° and 1.23 mm. The biggest variation of rotation in sagittal plane between two nearest lumbar spines is about 1°. Because of this displacement the frontal part of last mentioned disc is compressed with 530 N more and dorsal disc part as much less.

Key words: accelerometer, bicycling, biomechanical model, dynamics, spine

1. Introduction

Chronic Low Back Pain (LBP) is the most expensive benign case in industrialized countries and the most common cause for activity limitation among persons younger than 45 years. It is defined as pain that persists longer than 12 weeks and is often attributed to degenerative or traumatic conditions of the spine. Although acute LBP has a favorable prognosis, the effect of chronic LBP and its related disability on society is tremendous. Unlike acute LBP, chronic LBP serves no biologic purpose. However, it is a disorder that evolves in a complex milieu influenced by endogenous and exogenous factors, and it alters the individual's productivity to an extent beyond what the initiating pathologic dysfunction would [1]. The back represents by far the most common location for pain, with unspecified back pain effecting nearly a quarter of all respondents, lower back pain 18% and upper back pain 6% [2]. 75–80% of individuals in general population undergo it at least once during their life and 25% back pain becomes chronic. Chronic back pain causes permanent incapability of working and even may invalid the patient [3]. LBP and other spine diseases are common cyclist's problem, because they have to orient the spine in parallel with the horizontal plane for reaching the best aerodynamic position. Because of the back overload about 30% of cyclists after race have to be consulted by a physician. In following cases diagnosis is made as "undefined chronic pain" as a result of lack of spine biomechanics investigation [4]. Severe back pain most often arises from physical disruption of spine structures like intervertebral discs, epiphyseal joints and sacroiliac joints [5]. Prolonged flexed posture during cycling influences muscle fatigue and increased mechanical strain of the lumbar spine [6], [7]. Also riding surface unevenness can influence overall comfort during bicycle rides [8]. The aim of this study is to develop a dynamic model

of cyclist's lumbar region of the spine and evaluate the intervertebral distance variation which depends on wheeling regime and cyclist sitting position. The model can be used by bicyclist's investigators to see a relation between bicycle construction changes and load for human spine. Professional bicyclists also can use this model because the load for intervertebral discs depends on aerodynamic position and with dynamical model it is easy to find best choice between cyclist's posture, air resistance and fatigue during racing.

2. Materials and methods

Assuming that the main loading of the lumbar spine comes from the contact between bicycle seat and riders buttock during the riding on different surfaces and with different velocity, experimental measurements of the accelerations acting on the cyclist were performed. A 2-axial accelerometer ADXL320 was mounted on the seat-post of the bicycle so that sensitive axes were coincident with driving direction and vertical axis. Characteristics of acceleration (AC) measurements:

- AC measurement duration was 1 minute with different wheeling modes;
- AC sensor attached to the frontal plane at the bottom of the bicycle seat;
- Use of different wheeling surface modes: gravel road and asphalt road;
- Different tire pressure modes: 1.5 Bar and 3.5 Bar;
- Different wheeling speed modes: 10 km/h, 20 km/h, 30 km/h;
- Wireless speedometer-clock used to fix speed and wheeling duration;
- Each totally the same wheeling mode repeated at least 3 times;
- Experiment performed by a 23 year old, 73 kg of mass man (mass of bicycle ~ 7 kg);
- Measurement equipment was carried in the backpack (laptop with accelerometer interface).

By varying tire pressure and speed while driving on two different road surfaces various spine loading scenarios were evaluated. Wheeling mode was changed after at least 3 of the same mode trials (different wheeling modes: (1) gavel road, 10 km/h, 1.5 Bar; (2) gravel road, 20 km/h, 1.5 Bar; (3) gravel road, 30 km/h, 1.5 Bar; (4) old asphalt, 10 km/h, 3.5 Bar; etc.). With demonstrated wheeling modes it is possible to make 12 different measurements. Because of repeating each mode at least 3 times it is normal to perform at least 36 trials. The setup of the experimental measurements in moving bicycle is shown schematically in Fig. 1.
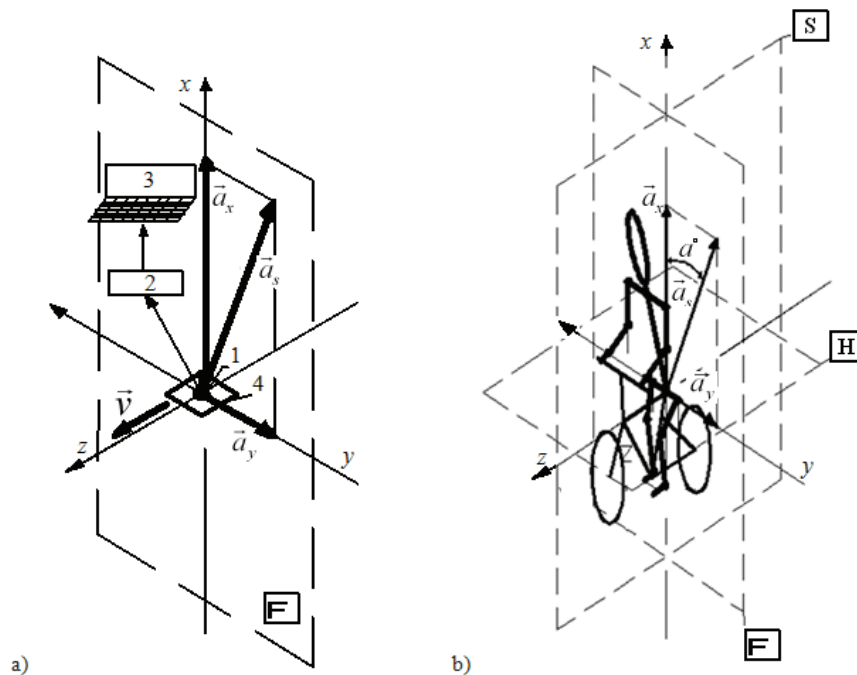

Fig. 1. Schematic accelerometer position during experiment: (a) accelerometer:
(1) position in frontal (F) plane: x and y – cross and vertical axes, 2 – portable data acquisition system,
3 – notebook, 4 – seat of bicycle, a_x, a_y – measured accelerations, $\overline{v}$ – driving direction;
(b) Schematic cyclist's drawing in space: H – horizontal plane, S – saggital plane, a_s – sum of vectors a_x and a_y
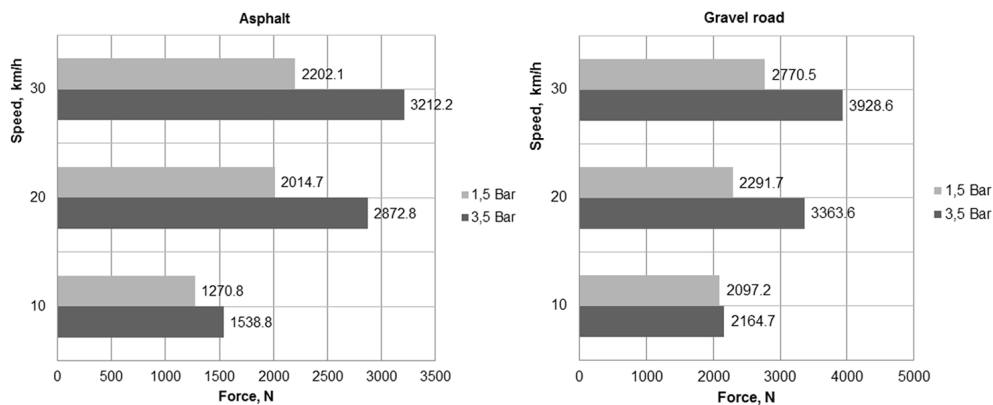
Fig. 2. Maximum force at the saddle during cycling on asphalt road and gravel road

During one minute of measurements there are few factors which influence excitation efficiency of "seat–buttock" system. Oscillations of the latter system depend on wheeling regimes (tires pressure, wheeling speed, road bumps). The largest discomfort during the transportation can arise mainly from low frequencies; therefore, data from accelerometers were recorded in time domain at a sampling frequency of 167 Hz. Then, spectral analysis of the acceleration data using discrete fast Fourier transformation in MATLAB software was performed. The spectral analysis of the frequency spectrum of the system's accelerations showed that dominant frequencies in measured data were in the range of 10–40 Hz. Acceleration signal was band-pass filtered using the 4th order Butterworth filter with 10–40 Hz cut-off frequency. The largest AC values in *x* and *y* axes were chosen for each wheeling regime. Finally, the dependence of measured external excitation forces on the wheeling regimes is demonstrated in Fig. 2.

External excitation frequencies could be confirmed because they satisfy other similar experiment results presented by Waechter et al. in 2002 [8]. Their studies demonstrated frequencies of about 0–50 Hz that dominated in measured data. In the last mentioned frequency interval there basically dominate all general AC and bigger frequency signals can be filtered to ensure elimination of noises and distortions. Also Waechter et al. defined resonance frequency interval of about 30–35 Hz at the back bicycle tree.

The higher the wheeling speed is, the larger force (almost 2 times) acts on lower back when tire pressure is constant. On average, the force is 1.4 times larger at higher tire pressure than at lower one. Also cyclists received bigger loads (about 1.2 times) during riding on uneven gravel road than on asphalt road of each wheeling regime. In order to investigate intervertebral linear and angular displacements a ten degrees of freedom dynamical model consisting of 5 lumbar region spine
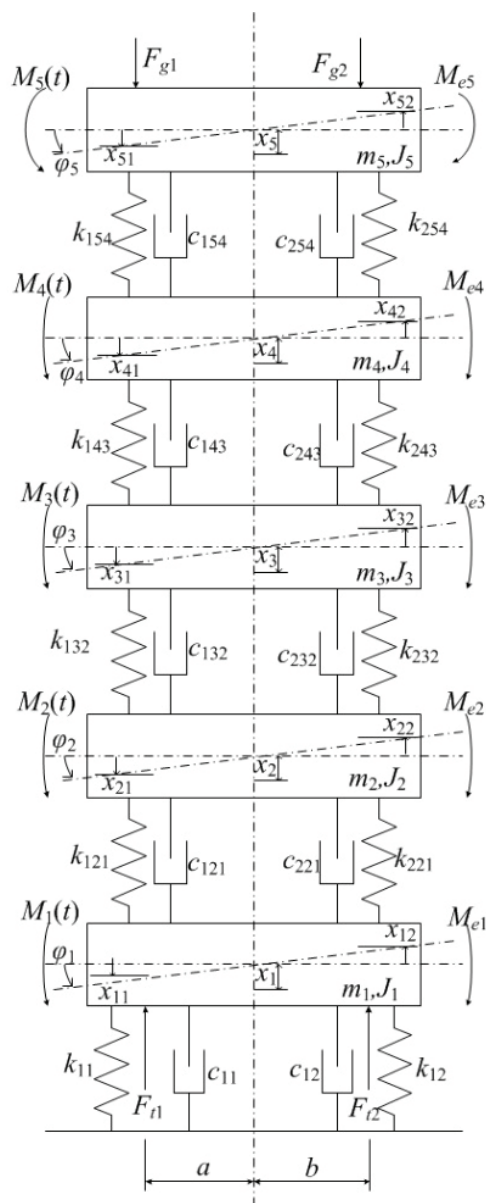

Fig. 3. Dynamic model of cyclist's spine lumbar region:
J_i – moments of inertia,
x_i – mass displacements, x_{i1}, x_{i2} – mass position variation because of rotation, $M_i(t)$ – external moments
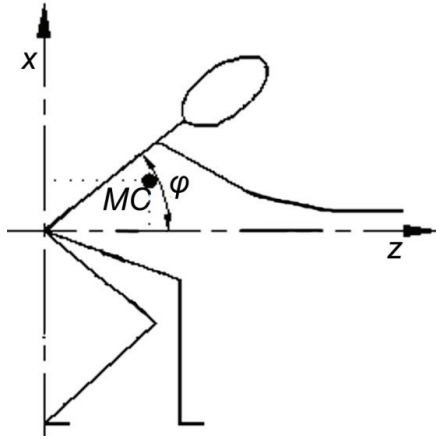
vertebrae was developed (Fig. 3) and the system of 10 second order differential equations of motion (1) was deduced using the Lagrange energy method. Experimentally determined load F_t with gravitation force F_g displace up and down by a distance x_i from the center of bodies whose masses are m_i. Also, bodies can rotate in sagittal plane at an angle φ_i about point O_i because of external moment of rotation M_i and moment of inertia M_{ei}. Calculated forces were used to load the mathematical model of spine. Intervertebral disc stiffness, damping constants [9] and vertebra's inertial characteristics [10] were chosen from scientific literature.

The seat influence on the outer force moment was evaluated. Cyclist's sitting position affects lumbar spine load subject to the spine inclination angle (Fig. 4), therefore three sitting positions were chosen: sport, middle and recreation.

External moment M_{ei} value due to the sitting position was used to load simulated biomechanical cyclist's spine model. In each case cyclist's coordinates of the center of mass (MC) were calculated (Table 1).

In every sitting posture in the center of mass of the upper torso the acts a gravitational force F_{MC}, which

$$
\left\{
\begin{aligned}
& m_1\ddot{x}_1 + \dot{x}_1\left(c_{121}+c_{221}+c_{12}+c_{11}\right) - \dot{x}_2\left(c_{121}+c_{221}\right) - \dot{\varphi}_1\left(c_{121}a+c_{11}a-c_{12}b-c_{221}b\right) - \dot{\varphi}_2\left(c_{221}b-c_{221}a\right) + \\
& +x_1\left(k_{121}+k_{11}+k_{221}+k_{12}\right) - x_2\left(k_{121}+k_{221}\right) - \varphi_1\left(k_{121}a+k_{11}a-k_{121}b-k_{12}b\right) + \varphi_2\left(k_{121}a-k_{221}b\right) = F_{t1}+F_{t2}, \\
& m_2\ddot{x}_2 - \dot{x}_1\left(c_{121}+c_{221}\right) + \dot{x}_2\left(c_{132}+c_{121}+c_{232}+c_{221}\right) - \dot{x}_3\left(c_{132}+c_{232}\right) + \dot{\varphi}_1\left(c_{121}a-c_{221}b\right) - \\
& -\dot{\varphi}_2\left(c_{232}a-c_{121}a-c_{232}b-c_{221}b\right) - \dot{\varphi}_3\left(c_{232}b-c_{132}a\right) - x_1\left(k_{121}+k_{221}\right) + x_2\left(k_{132}+k_{121}+k_{232}+k_{221}\right) + \\
& +x_3\left(k_{132}+k_{232}\right) - \varphi_1\left(k_{121}a-k_{221}b\right) + \varphi_2\left(k_{132}a+k_{121}a-k_{232}b-k_{221}b\right) + \varphi_3\left(k_{132}a-k_{232}b\right) = 0, \\
& m_3\ddot{x}_3 - \dot{x}_2\left(c_{132}+c_{232}\right) + \dot{x}_3\left(c_{143}+c_{132}+c_{243}+c_{232}\right) - \dot{x}_4\left(c_{143}+c_{243}\right) - \dot{\varphi}_2\left(c_{232}b-c_{132}a\right) - \\
& -\dot{\varphi}_3\left(c_{143}a+c_{132}a-c_{243}b-c_{232}b\right) - \dot{\varphi}_4\left(c_{243}b-c_{143}a\right) - x_2\left(k_{132}+k_{232}\right) + x_3\left(k_{143}+k_{132}+k_{232}+k_{243}\right) \\
& -x_4\left(k_{143}+k_{243}\right) - \varphi_2\left(k_{232}b-k_{132}a\right) - \varphi_3\left(k_{143}a+k_{132}a-k_{232}b-k_{243}b\right) - \varphi_4\left(k_{243}b-k_{143}a\right) = 0, \\
& m_4\ddot{x}_4 - \dot{x}_3\left(c_{143}+c_{243}\right) + \dot{x}_4\left(c_{154}+c_{143}+c_{254}+c_{243}\right) - \dot{x}_5\left(c_{154}+c_{254}\right) - \dot{\varphi}_3\left(c_{243}b-c_{143}a\right) - \\
& -\dot{\varphi}_4\left(c_{154}a+c_{143}a-c_{254}b-c_{243}b\right) - \dot{\varphi}_5\left(c_{254}b-c_{154}a\right) - x_3\left(k_{143}+k_{243}\right) + x_4\left(k_{154}+k_{143}+k_{254}+k_{243}\right) \\
& -x_5\left(k_{154}+k_{254}\right) - \varphi_3\left(k_{243}b-k_{143}a\right) - \varphi_4\left(k_{154}a+k_{143}a-k_{254}b-k_{243}b\right) + \varphi_4\left(k_{254}b-k_{154}a\right) = 0, \\
& m_5\ddot{x}_5 - \dot{x}_4\left(c_{154}+c_{254}\right) + \dot{x}_5\left(c_{154}+c_{254}\right) - \dot{\varphi}_4\left(c_{254}b-c_{154}a\right) - \dot{\varphi}_5\left(c_{154}a+c_{254}b\right) - x_4\left(k_{154}+k_{254}\right) + \\
& +x_5\left(k_{154}+k_{254}\right) - \varphi_4\left(k_{254}b-k_{154}a\right) - \varphi_5\left(k_{154}a-k_{254}b\right) = -F_{g1}-F_{g2}, \\
& J_1\ddot{\varphi}_1 - \dot{x}_1\left(c_{121}a+c_{221}b+c_{11}a+c_{12}b\right) + \dot{x}_2\left(c_{121}a-c_{221}b\right) + \dot{\varphi}_1\left(c_{121}a^2+c_{11}a^2+c_{221}b^2+c_{12}b^2\right) - \\
& -\dot{\varphi}_2\left(c_{121}a^2+c_{221}b^2\right) - x_1\left(k_{121}a+k_{11}a-k_{221}b-k_{12}b\right) + x_2\left(k_{121}a-k_{221}b\right) + \\
& +\varphi_1\left(k_{121}a^2+k_{11}a^2+k_{221}b^2+k_{12}b^2\right) - \varphi_2\left(k_{121}a^2+k_{221}b^2\right) = M_1-F_{t1}a+F_{t2}b, \\
& J_2\ddot{\varphi}_2 - \dot{x}_2\left(c_{132}a+c_{121}a-c_{232}b-c_{221}b\right) + \dot{x}_1\left(c_{121}a-c_{221}b\right) + \dot{x}_3\left(c_{132}a-c_{232}b\right) - \dot{\varphi}_1\left(c_{121}a^2+c_{221}b^2\right) + \\
& +\dot{\varphi}_2\left(c_{132}a^2+c_{121}a^2+c_{232}b^2+c_{221}b^2\right) - \dot{\varphi}_3\left(c_{132}a^2+c_{232}b^2\right) + x_1\left(k_{121}a-k_{221}b\right) - x_2\left(k_{132}a+k_{121}a-k_{232}b-k_{221}b\right) + \\
& +x_3\left(k_{132}a-k_{232}b\right) - \varphi_1\left(k_{121}a^2+k_{221}b^2\right) + \varphi_2\left(k_{132}a^2+k_{121}a^2+k_{232}b^2+k_{221}b^2\right) - \varphi_3\left(k_{132}a^2+k_{232}b^2\right) = M_2, \\
& J_3\ddot{\varphi}_3 + \dot{x}_2\left(c_{132}a-c_{232}b\right) - \dot{x}_3\left(c_{143}a+c_{132}a-c_{243}b-c_{232}b\right) + \dot{x}_4\left(c_{143}a-c_{232}b\right) - \dot{\varphi}_2\left(c_{132}a^2+c_{232}b^2\right) + \\
& +\dot{\varphi}_3\left(c_{143}a^2+c_{132}a^2+c_{243}b^2+c_{232}b^2\right) - \dot{\varphi}_4\left(c_{143}a^2+c_{243}b^2\right) + x_2\left(k_{132}a-k_{232}b\right) - x_3\left(k_{143}a+k_{132}a-k_{232}b-k_{243}b\right) + \\
& +x_4\left(k_{143}a-k_{243}b\right) - \varphi_2\left(k_{132}a^2+k_{232}b^2\right) + \varphi_3\left(k_{143}a^2+k_{132}a^2+k_{232}b^2+k_{243}b^2\right) - \varphi_4\left(k_{143}a^2+k_{243}b^2\right) = M_3, \\
& J_4\ddot{\varphi}_4 + \dot{x}_3\left(c_{143}a-c_{243}b\right) - \dot{x}_4\left(c_{154}a+c_{143}a-c_{254}b-c_{243}b\right) + \dot{x}_5\left(c_{154}a-c_{254}b\right) - \dot{\varphi}_3\left(c_{143}a^2+c_{243}b^2\right) + \\
& +\dot{\varphi}_4\left(c_{154}a^2+c_{143}a^2+c_{254}b^2+c_{243}b^2\right) - \dot{\varphi}_5\left(c_{154}a^2+c_{254}b^2\right) + x_3\left(k_{143}a-k_{243}b\right) - x_4\left(k_{154}a+k_{143}a-k_{254}b-k_{243}b\right) + \\
& +x_5\left(k_{154}a-k_{254}b\right) - \varphi_3\left(k_{143}a^2+k_{243}b^2\right) + \varphi_4\left(k_{154}a^2+k_{143}a^2+k_{254}b^2+k_{243}b^2\right) - \varphi_5\left(k_{154}a^2+k_{254}b^2\right) = M_4, \\
& J_5\ddot{\varphi}_5 + \dot{x}_4\left(c_{154}a-c_{254}b\right) + \dot{x}_5\left(c_{254}b-c_{154}a\right) - \dot{\varphi}_4\left(c_{154}a^2+c_{254}b^2\right) + \dot{\varphi}_5\left(c_{154}a^2+c_{254}b^2\right) + \\
& +x_4\left(k_{154}a-k_{254}b\right) + x_5\left(k_{254}b-k_{154}a\right) - \varphi_4\left(k_{154}a^2+k_{254}b^2\right) + \varphi_5\left(k_{154}a^2+k_{254}b^2\right) = M_5+F_{g1}a-F_{g2}b.
\end{aligned}
\right.
\tag{1}
$$

Fig. 4. Cyclist's sitting position subject to spine angle φ

force F_{compr}. We assume that this force is distributed evenly on the facet surface of the vertebra (Fig. 6).

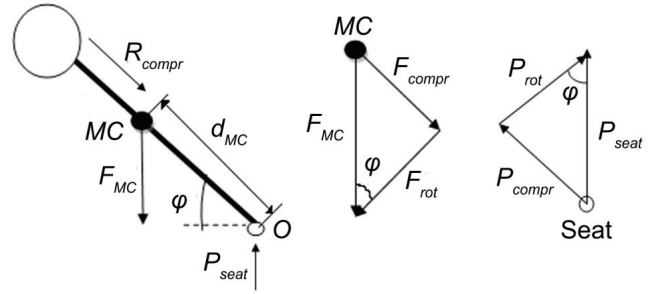Fig. 5. Schematics for the evaluation of dynamic loading of the vertebra

has two constituents – rotational and compressive (Fig. 5). The rotational F_{rot} component creates a torque about the point O, which is the point of bicyclist's support against saddle, and compressive force F_{compr}, which is acting perpendicularly to facet surface of the vertebrae (Fig. 6). To counterbalance this gravitational force F_{MC}, the spinal muscles must create force F_R, which can be estimated from the moments balance equation,

$$F_R = \frac{d_{MC} \cdot F_{rot}}{d_R} \qquad (2)$$

where d_R is the arm of the muscle force and based on spine morphology it is approximately equal to 30 mm, d_{MC} – arm of a gravitational force and it is estimated from the coordinates of body mass center depending on the sitting posture (Table 1). Because of this muscle force, the vertebrae of the spine are compressed more and the bigger the arm of the force, the bigger the compressive force is. Thus, the sitting posture influences the loading of the lumbar spine. As can be concluded from the equation (2), the muscle force depends on the ratio of force arm d_{MC}/d_R.

Total force that acts on L1 vertebra is expressed as the sum of muscle force F_R and compressive
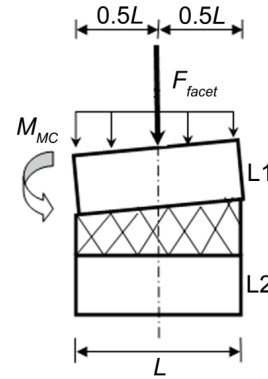

Fig. 6. Concentrated load acting on L1 facet surface of the vertebra

For every sitting position the calculated parameters are provided in Table 2.

The loads described above due to gravitational forces are not enough to estimate intervertebral displacements in the dynamic model during different wheeling regimes and sitting postures. In order to evaluate changes in intervertebral distances from the external excitation forces it is required to account the response of lumbar part to the dynamic motion, which

Table 1. Coordinates of cyclists of MC according to sitting position

Sitting type\MC coordinates	x_c, m	y_c, m	z_c, m
Sport ($\varphi = 38°$)	0.1485	0	0.3103
Middle ($\varphi = 60°$)	0.2309	0	0.2027
Recreation ($\varphi = 80°$)	0.2727	0	0.0874

Table 2. Estimated parameters of forces and moments

Sitting posture\parameter	d_{MC}, m	F_{rot}, N	M_{MC}, Nm	F_{compr}, N	F_R, N	F_{facet}, N
Recreational	0.29	79.14	22.95	448.85	573.75	1022.6
Middle	0.31	227.89	70.65	394.71	1766.25	1994.14
Sport	0.34	359.15	122.11	280.60	3052.75	3333.35

creates additional force on the vertebrae. During the experimental measurements of accelerations force P_{seat} acting on the saddle was estimated and it is equal to the measured acceleration times the mass of the bicyclist above the seat. This saddle force consists of two elements – lumbar compressive force P_{compr} and rotation causing P_{rot}. Compressive force P_{compr} in the dynamic model is taken as reaction force R_{compr} due to inertia of the torso, and therefore this reaction force is added to static force F_{facet} and so the total force F_{total} acting on the lumbar spine vertebrae is equal to

$$F_{total} = F_{facet} + R_{compr} . \qquad (3)$$

3. Results

The developed dynamic model of lumbar spine enabled us to calculate intervertebral linear and angular displacements in sagittal plane. The biggest linear and angular displacements were found between L4–L5 vertebras. This is because of the increase of a moment arm and concentration of mass at this place. Figure 8a demonstrates the biggest linear displacement between two nearest lumbar vertebras during particular wheeling regime subject to sitting position. Here the biggest change of distance is shown after the maximum (3.5 Bar; 30 km/h) and
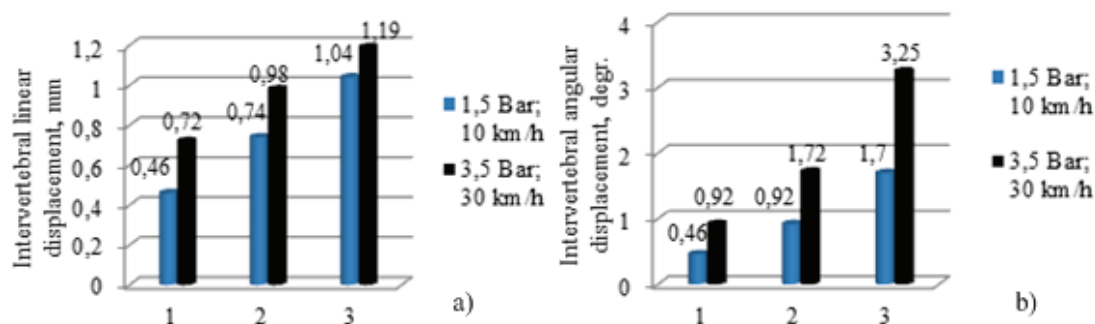

Fig. 7. One of the load function shapes used to investigate dynamic response of a model

Thus, the rotational component P_{rot} forms a rotation moment $M_{P_{rot}}$ about MC when the arm of the force is d_{CM}. Total rotation moment as a sum of rotation moments $M_{P_{rot}}$ due to the external excitation force and rotation moment M_{MC} due to the gravitational forces in the system of equations (1) is denoted by M_5. For solution of the equations of motion (1) a variable order method based on numerical differentiation formulas, which is designed specifically to deal with stiff differential systems of equations, was used. Optionally it uses the backward differentiation formulas. This method helped to calculate 10 unknown parameters of the simulated system solid bodies': 5 linear displacements and 5 angular displacements during each wheeling regime and sitting position at cycling. To research the response of the dynamical model subject to various loads with different magnitude and duration, following scenarios for loading functions were used: (1) same amplitude but different duration impulse time (Fig. 7); (2) same time duration but different amplitude impulses; (3) shape of sin and cos functions; (4) constant load all the time.

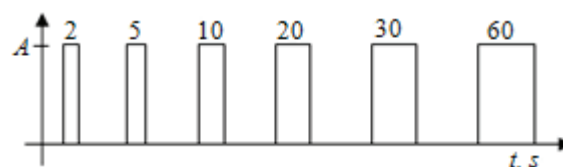minimum (1.5 Bar; 10 km/h) wheeling load conditions.

Fig. 8. Largest intervertebral linear (a) and angular (b) displacements during wheeling depending on cycling regime and sitting position: recreation (1), middle (2), sport (3)

It can be concluded that the bigger the spine bend angle φ is, the lower the linear intervertebral distance change. Also, simulated model shows correctly dependence between wheeling regimes and the load that acts on the spine. Simulated model shows that the bigger the cyclist's speed or pressure in the tires, the higher the angular displacements to lumbar spine vertebrae. Also, it is visible how a vertebra rotation angle is changing during different sitting positions, i.e., because of longer MC coordinate z. In Fig. 9,
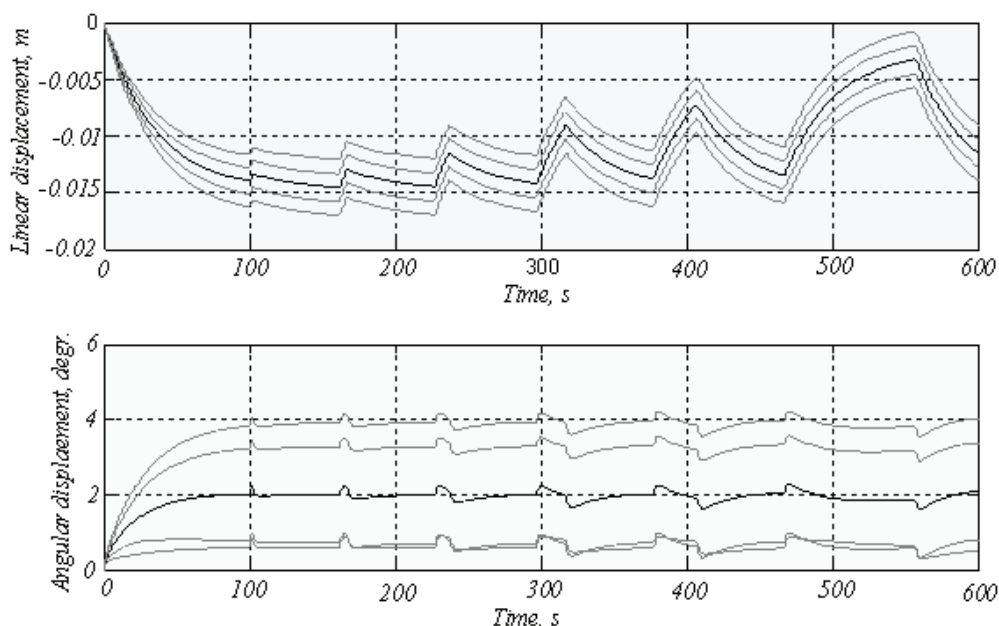
Fig. 9. Dynamical model response under impulsive loads (2 s, 5 s, 10 s, 20 s, 30 s, 90 s)
during cycling on gravel road at the speed of 30 km/h, tire pressure 3.5 Bar and sitting position – sport

a response of dynamic model to impulsive loads is presented. It can be seen that dynamical model has 100 sec delay from the loading start till the structure reaches stable condition under compression. Also it is visible that when impulse duration is less than 1 sec, the model linear and angular displacements are almost negligible.

At 30 km/h speed and 3.5 Bar tyre pressure the cyclist's lumbar spine suffers maximum loads which are approximately 3212.2 N parallel to the x axis during wheeling on asphalt and 3928.6 N during wheeling on public road. During wheeling the external frequency distributes in range from 10 Hz to 40 Hz. The biggest load protractile spine muscle experiences in the sport sitting position. Maximum vertebrae rotation and linear variation values in wheeling regime with 1.5 Bar tyre pressure and at 10 km/h speed are 0.46° and 0.46 mm. Maximum vertebrae rotation and linear variation values at wheeling regime with 3.5 Bar tyre pressure and at 30 km/h speed are 3.9° and 1.23 mm. The biggest variation of rotation in sagittal plane between two nearest lumbar spine is about 1°. Because of this displacement the frontal part of the last mentioned disc is compressed with 530 N more and dorsal disc part as much less.

About 2–4 kN compressive force [11] loaded two nearest intact L4–L5 vertebrae and intervertebral lumbar discs deformation in 1–2 mm interval was fixed [11]. During sagittal angular displacement 1 kN compressive force and small 2–10 Nm sagittal bending moment loaded two adjacent L4–L5 vertebrae. At this time angular displacement is in the interval 2–6° [11]. This linear deformation is comparable to that calculated by our dynamical model – 3.9 kN and 1.23 mm and a little bit different angular displacement could be obtained because of dissimilar compressive force and bending moment relation. So, we can confirm the fact that the results calculated using the biomechanical lumbar spine model presented in this paper agree with experimentally measured values obtained by other authors.

4. Discussion

While analysing various scientific articles on the topic, it became clear that the research object is usually a part of a spine column, which is affected by static load, torque or combined loading. In all the cases analysed the general investigations of loads occurring in spine vertebrae are performed when the nature of the loading is unknown and in most cases this loading is static. Most scientific works are intended for dynamic loading research of overall effect of vibrations and bicycle' structural parts on the human body. Therefore, the main motivation for our research was to perform investigation of the impact on the spine and to carry it out in different way, i.e., by selecting particular loading nature to measure its dynamic constituent and focus on the analysis of loads occurring in the lumbar region of the spine. Waechter

et al. [8] were performing a research on the design of vibration dampers for a bicycle and they estimated experimentally dominant frequencies in the range from 0 to 50 Hz. In this frequency range they found that resonant frequency at the back of the bicycle range from 30 to 35 Hz. In our case, the spectral analysis of the frequency spectrum of the system accelerations showed that dominant frequencies in measured data were in the range of 10–40 Hz and it follows that our method is appropriate to estimate external excitation forces from the accelerations in this frequency range. Bicyclists tend to increase their speed by taking particular body posture in order to minimize aerodynamic drag and maximize exerted forces; however, this may lead to pains in the spine and neck regions. According to Mestdagh [7], Salai [4] et al., overall bicyclist' posture influences physiological condition of the spine, and especially neck and lumbar regions. Adams et al. [5] were among the first who attempted to analyze back pains and disturbances and suggested future opportunities for biomechanics. Studies show that severe back pain most often arises from physical disruption of intervertebral discs from mechanical loading. According to Adams, suggested priority areas for future research should include understanding interactions between intervertebral discs and adjacent vertebrae. Therefore, we believe that our dynamic model of five lumbar spine vertebrae despite its simplifications and limitations would allow us to investigate intervertebral interactions under the action of impulsive mechanical loads. It was estimated that the intervertebral distances vary due to an increase of dynamic loading and sitting posture. For the future research it is possible to develop a methodology for estimating how much time and in what regime it is healthier to ride by calculating average weighed acceleration value based on ISO 2631.

References

[1] Wheeler A.H., *Pathophisiology of Chronic Back pain*, Headache and Pain, 2007, Vol. 07(9), 1–15.

[2] Hunt T., *Pain in Europe – A report*, Cambridge University, 2007, 24.

[3] Valeikiene V., Mercekas G., *Acute and chronic back pain of older patients, Gerontologija*, 2006, Vol. 7(3), 154–157.

[4] Salai M., Brosh T., Blankstein A., Oran A., Chechik A., *Effect of changing the saddle angle on the incidence of low back pain in recreational cyclists*, Br. J. Sports Med., 1999, Vol. 33(6), 398–400.

[5] Adams M.A., Dolan P., *Spine biomechanics*, J. Biomech., 2005, Vol. 38(10), 1972–1983.

[6] Mardsen M., Schwellnus M., *Lower back pain in cyclists: A review of epidemiology, pathomechanics and risk factors*, Int. J. Sports Med., 2010, Vol. 11(1), 216–225.

[7] Vey Mestdagh K., *Personal perspective: in search of an optimum cycling posture*, Appl. Ergon. J., 1998, Vol. 5(29), 325–334.

[8] Waechter M., Riess F., Zacharias N., *A multibody model for the simulation of bicycle suspension systems*, Vehicle systems dynamics, 2002, Vol. 37(1), 3–28.

[9] Kurutz M., *In vivo age- and sex-related creep of human lumbar motion segments and discs in pure centric tension*, J. Biomech., 2006, Vol. 39(7), 1180–1190.

[10] Gardner-Morse M., Stokes I., *Structural behaviour of human lumbar spinal motion segments*, J. Biomech., 2004, Vol. 37(2), 205–212.

[11] Borkowski P., Marek P., Krzesinski G. et al. *Finite element analysis of artificial disc with an elastomeric core in the lumbar spine*, Acta Bioeng. Biomech., 2012, Vol. 14(1), 1–8.